

## MIT Open Access Articles

*Bioinorganic Explorations of Zn(II) Sequestration  
by Human S100 Host-Defense Proteins*

The MIT Faculty has made this article openly available. **Please share**  
how this access benefits you. Your story matters.

**Citation:** Cunden, Lisa S., and Elizabeth M. Nolan. "Bioinorganic Explorations of Zn(II) Sequestration by Human S100 Host-Defense Proteins." *Biochemistry* 57, 11 (January 2018): 1673-1680 © 2018 American Chemical Society

**As Published:** <http://dx.doi.org/10.1021/acs.biochem.7b01305>

**Publisher:** American Chemical Society (ACS)

**Persistent URL:** <https://hdl.handle.net/1721.1/123659>

**Version:** Author's final manuscript: final author's manuscript post peer review, without publisher's formatting or copy editing

**Terms of Use:** Article is made available in accordance with the publisher's policy and may be subject to US copyright law. Please refer to the publisher's site for terms of use.





Published in final edited form as:

Biochemistry. 2018 March 20; 57(11): 1673–1680. doi:10.1021/acs.biochem.7b01305.

## Bioinorganic Explorations of Zn(II) Sequestration by Human S100 Host-Defense Proteins

Lisa S. Cunden<sup>1</sup> and Elizabeth M. Nolan<sup>1,\*</sup>

<sup>1</sup>Department of Chemistry, Massachusetts Institute of Technology, Cambridge, MA 02139, United States

### Abstract

The human innate immune system launches a metal-withholding response to starve invading microbial pathogens of essential metal nutrients. Zn(II)-sequestering proteins of the human S100 family contribute to this process and include calprotectin (CP, S100A8/S100A9 oligomer, calgranulin A/B oligomer), S100A12 (calgranulin C), and S100A7 (psoriasin). This perspective highlights recent advances on the Zn(II) coordination chemistry of these three proteins, as well as select studies that evaluate Zn(II) sequestration as an antimicrobial mechanism.

### Graphical Abstract



Zn(II) is a ubiquitous d-block metal ion that performs structural, catalytic, and signaling roles in biology.<sup>1,2</sup> In the context of the host/microbe interaction and infectious disease, invading microbial pathogens must obtain this essential metal nutrient from the host to colonize and promote virulence.<sup>3,4</sup> The mammalian innate immune system, which provides a first line of defense against pathogenic invaders, employs one of two opposing strategies to modulate Zn(II) levels at infection sites and thereby inhibit the growth of pathogens: Zn(II) limitation and Zn(II) intoxication.<sup>4,5</sup> This perspective focuses on the former phenomenon, which is a component of the metal-withholding innate immune response. This process is often termed “nutritional immunity.”<sup>6–8</sup> In response to Zn(II) limitation and in an attempt to fulfill their nutritional requirements, pathogens express high-affinity Zn(II)-uptake systems to acquire Zn(II) from the host environment.<sup>4,5,9,10</sup> Thus, a tug-of-war for a limited supply of metal nutrient occurs at the host/pathogen interface, and the outcome of this competition impacts the progression of infection. Zn(II)-sequestering host-defense proteins are important contributors to this host/microbe interaction and, in humans, include three proteins from the S100 family: calprotectin (CP, S100A8/S100A9 oligomer, calgranulin A/B oligomer), S100A12 (calgranulin C), and S100A7 (psoriasin) (Figures 1, 2).

\*Corresponding author: lnolan@mit.edu, Phone: 617-452-2495.

Human S100 proteins include 21 relatively small ( $\approx 10$  kDa)  $\alpha$ -helical Ca(II)-binding polypeptides.<sup>11</sup> Apo S100 proteins typically exist as homodimers, or as a heterodimer in the case of CP, that each form a stable four-helix domain with a hydrophobic core. Each S100 polypeptide contains two EF-hand domains where the C-terminal EF-hand is described as “canonical” or “calmodulin-like” and the N-terminal EF-hand is described as “non-canonical.” A “canonical” EF-hand domain affords a heptadentate coordination sphere for Ca(II), whereas a “non-canonical” EF-hand binds Ca(II) with lower coordination number.<sup>12</sup> A comparison of the structures of CP, S100A12, and S100A7 highlights some additional similarities (Figures 2, 3). Each hetero- or homodimer exhibits two transition-metal-binding sites that are independent from the Ca(II)-binding sites. The transition-metal-binding sites form at the homo- or heterodimer interface and are composed of two or more metal-binding residues from each subunit. Despite these commonalities, biological and biochemical studies performed over the past three decades have demonstrated that each protein exhibits distinct expression patterns, as well as Zn(II)-binding and -sequestering strategies.

Human CP is produced and released by white blood cells and epithelial cells.<sup>13,14</sup> Neutrophils constitutively express CP, which constitutes  $\approx 40\%$  of total cytoplasmic protein in these immune cells. Monocytes and macrophages also express this protein.<sup>15,16</sup> Apo CP exists as a heterodimer of S100A8 ( $\alpha$ , 10.8 kDa) and S100A9 ( $\beta$ , 13.2 kDa). Coordination of Ca(II) ions at the EF-hand domains, or a divalent transition metal ion at the His<sub>6</sub> site, causes two heterodimers to self-associate and form a heterotetramer.<sup>17–21</sup> CP exhibits broad-spectrum antimicrobial activity, and early studies identified a link between its growth inhibitory activity and Zn(II).<sup>22–26</sup> More recent investigations have (i) defined how CP contributes to Zn(II) sequestration,<sup>27,28</sup> (ii) examined how select microbial pathogens respond to Zn(II) limitation imposed by CP,<sup>29–33</sup> and (iii) uncovered that CP can withhold additional divalent first-row transition metals, including Mn(II),<sup>34–36</sup> Fe(II),<sup>37</sup> Ni(II),<sup>38</sup> and Cu(II).<sup>39</sup>

Human S100A12 is also produced and released by neutrophils.<sup>40,41</sup> This protein is abundant, at least based on studies of porcine neutrophils, where it was found to constitute up to 8% of total cytoplasmic protein.<sup>42</sup> Other white blood cells that include monocytes, macrophages and eosinophils, as well as epithelial cells, also express S100A12.<sup>43–48</sup> It is a 21-kDa homodimer that self-associates into tetramers and hexamers in the presence of metal ions.<sup>49–53</sup> S100A12 is accepted to participate in nutritional immunity, and the current model suggests that it selectively sequesters Zn(II).<sup>54,55</sup> It exhibits antifungal activity against *Candida* spp and antibacterial activity against some pathogens including *Listeria monocytogenes*.<sup>54,55</sup>

Human S100A7 (psoriasin) is a 22-kDa homodimer that is expressed by epithelial cells and secreted into the upper epithelia.<sup>56–59</sup> In contrast to CP and S100A12, higher-order oligomers of S100A7 have not been observed. S100A7 has been identified as an antibacterial factor of the skin,<sup>60</sup> tongue,<sup>61</sup> and female genital tract.<sup>62</sup> Recent studies reported that S100A7 possesses antifungal activity.<sup>63</sup> To date, three different mechanisms of action have been proposed for the host-defense function of S100A7, one of which involves Zn(II) sequestration.<sup>60,64</sup>

Beyond participating in the metal-withholding response, S100 proteins have been associated with a variety of intracellular and extracellular processes, including cytoskeletal interactions, protein phosphorylation, membrane trafficking, calcium homeostasis, cell growth and migration, regulation of the cell cycle and transcription factors, tissue development and repair, cell migration and chemotaxis, and innate and adaptive immune responses.<sup>11,65,66</sup> Metal ions have been shown to mediate some of these processes, including the interaction of S100A12 with the receptor for advanced glycosylated end products (RAGE), which triggers a proinflammatory response.<sup>67</sup> While these topics are outside of the scope of this review, we look forward to future studies that address how transition metal ions contribute to the functions of S100 proteins in a variety of contexts.

In the following sections, we present a selection of recent work that has advanced our knowledge of the Zn(II)-binding properties of human CP, S100A12 and S100A7. Together, these vignettes describe new facets of the biological coordination chemistry of Zn(II) and inform our molecular understanding of how S100 proteins contribute to innate immunity, the host/microbe interaction, and the homeostasis of metal ions.

### Calprotectin (S100A9/S100A9 Oligomer)

Among the Zn(II)-chelating S100 proteins, CP is unique because of its heterooligomeric (S100A8/S100A9) composition. This structural attribute affords four different EF-hand domains and two transition metal-binding sites with different amino acid compositions per heterodimer (Figure 2A–C). Moreover, S100A9 is the longest human S100 polypeptide and it exhibits a C-terminal extension or “tail” that we define as residues 96–114 (Figure 3). These unusual features define the coordination chemistry of CP and its remarkable metal-sequestering ability. The transition-metal-binding sites are located at the S100A8/S100A9 heterodimer interface and are commonly referred to as site 1 and site 2. Site 1 is a His<sub>3</sub>Asp motif composed of His83 and His87 from S100A8, and His20 and Asp30 from S100A9 (Figure 2C). Site 2 is a biologically unprecedented His<sub>6</sub> motif defined by His17 and His27 from S100A8, and His91, His95, His103, and His105 from S100A9 (Figure 2C).<sup>28,37,38,68–70</sup> His103 and His105 are located in the flexible C-terminal tail of the S100A9 subunit. Both sites coordinate Zn(II) with high affinity and provide a 2:1 Zn(II):CP heterodimer stoichiometry, as described further below. Because no crystallographic or solution structure of Zn(II)-bound CP has been reported to date, current understanding of Zn(II) chelation by CP is based on results from solution studies.

A recent investigation established that the Zn(II) ion coordinated at site 2 is ligated by the six residues of the His<sub>6</sub> motif.<sup>28</sup> Prior to this work, it was unclear whether His103 and His105 of the S100A9 C-terminal tail contribute to Zn(II) binding at this site. During investigations of the protease stability of CP, a serendipitous observation provided compelling evidence for the existence of an unprecedented Zn(II)-His<sub>6</sub> site. Whereas proteinase K cleaved the S100A9 polypeptide of Ca(II)-bound CP after His104, addition of 2 equivalents of Zn(II) protected this cleavage site.<sup>21</sup> When the CP variants His103Ala and His105Ala were examined, proteinase K cleaved the S100A9 subunit of the Zn(II)-free and Zn(II)-bound protein after His104, suggesting that both His103 and His105 are involved in coordinating Zn(II) at site 2. This notion was supported by X-ray absorption spectroscopy of

the Zn(II)-bound His<sub>3</sub>Asp variant of CP, which has the four residues of the His<sub>3</sub>Asp site mutated to Ala residues. The X-ray absorption near-edge structure (XANES) region of the spectrum indicated that the Zn(II) ion is coordinated in a six-coordinate geometry, and the extended X-ray absorption fine structure (EXAFS) region was consistent with Zn(II) in a His<sub>6</sub> coordination environment.<sup>28</sup> This result is consistent with studies of Mn(II), Fe(II) and Ni(II) coordination at this site; the promiscuous His<sub>6</sub> motif allows CP to compete with microbes for multiple divalent first-row transition metal ions.<sup>37,38,68,69</sup> The coordination number of Zn(II) bound at the His<sub>3</sub>Asp site is currently unclear and a topic for future investigation. In particular, whether the Asp residue is mono- or bidentate is unknown.

A variety of experiments have been performed to ascertain the Zn(II)-binding affinities of sites 1 and 2, including direct Zn(II)-binding titrations monitored by isothermal titration calorimetry (ITC) and Zn(II) competition titrations (Table 1). In the latter experiments, a fluorescent small-molecule Zn(II) sensor of known Zn(II)-binding affinity (apparent dissociation constant value,  $K_{d,Zn(II)}$ ) and CP are allowed to compete for Zn(II), and the fluorescence observed from the sensor provides a quantitative measure of the relative affinities of the two competitors. Because CP also binds Ca(II) ions, titrations with Ca(II)-insensitive Zn(II) sensors are important for interrogating the effect of Ca(II) ions on Zn(II) binding. In early work, the Ca(II)-insensitive sensor Zinpyr-4 (ZP4,  $K_{d,Zn(II)} = 650$  pM, pH 7.0)<sup>72</sup> revealed that Ca(II) ions modulate the Zn(II) affinities of both sites 1 and 2 (Table 1).<sup>28</sup> In particular, ZP4 showed that Ca(II)-bound CP coordinates Zn(II) with higher affinity than the Ca(II)-free form. This discovery provided the foundation for the current model where the Ca(II) ion concentrations in the cytoplasm and extracellular space modulate the functional properties of CP (*vide infra*).<sup>27</sup>

One limitation of the ZP4 competition experiments was that CP outcompeted ZP4 for Zn(II) in the presence of excess Ca(II) ions; thus, only upper limits to the Zn(II) affinities could be determined from this method. Later, a new fluorescent Ca(II)-insensitive Zn(II) sensor named HNBO-DPA that binds Zn(II) with higher affinity than ZP4 was reported (HNBO-DPA  $K_{d,Zn(II)} = 12$  pM, pH 7.0).<sup>73</sup> Competition experiments performed with HNBO-DPA provided a new set of  $K_{d,Zn(II)}$  values of Ca(II)-bound CP, and indicated that Ca(II)-insensitive Zn(II) sensors with greater Zn(II) affinity are needed because one Zn(II)-binding site out-competed HNBO-DPA for Zn(II) (Table 1).<sup>28</sup> Moreover, Zn(II) competition titrations with HNBO-DPA and a variant of CP that has no His residues in the S100A9 C-terminal tail (His103Ala/His104Ala/His105Ala variant) provided two additional important insights: (i) the tail His residues of CP contribute to high-affinity Zn(II) binding at the His<sub>6</sub> site and (ii) perturbation of the His<sub>6</sub> site lowered the Zn(II) affinity of the His<sub>3</sub>Asp site. The latter observation provided the first hint of allostery between sites 1 and 2.<sup>28</sup> Further defining the Zn(II)-binding affinities, assessing the binding order, and deciphering crosstalk between the His<sub>3</sub>Asp and His<sub>6</sub> sites are avenues that warrant continued investigation. In summary, the  $K_{d,Zn(II)}$  values determined for CP to date are consistent with its role as a Zn(II)-sequestering host-defense protein. Indeed, recent work demonstrated that both sites 1 and 2 of CP sequester Zn(II) from microbes and thereby contribute to its growth inhibitory properties.<sup>28</sup>

As noted above, one major finding from the initial Zn(II) competition studies with ZP4 was that the presence of excess Ca(II) ions enhances the Zn(II) affinities of both sites 1 and 2.<sup>27</sup> This work, as well as subsequent studies of how CP coordinates other divalent transition metals,<sup>36,37,74</sup> indicated that CP morphs into its high-affinity, metal-sequestering form in the extracellular milieu where Ca(II) concentrations are orders of magnitude higher than those found in the cytoplasm of resting cells (e.g. 10–100 nM versus  $\approx$ 2 mM). The molecular basis for how Ca(II) complexation enhances the Zn(II) affinities requires elucidation. Ca(II) binding causes formation of S100A8/S100A9 tetramers<sup>17–19</sup> and enhances the proteolytic stability of the protein,<sup>21</sup> which suggests that changes in conformation or dynamics may be at work. These observations also suggest that CP is predominantly a heterodimer when stored in the cytoplasm and forms heterotetramers in the extracellular space (Figure 1). In agreement with the notion that Ca(II) ions enhance metal sequestration, several studies have shown that the presence of Ca(II) ions enhances the ability of CP to deplete transition metals from microbial growth medium and its antimicrobial activity.<sup>27,28,34,37,75</sup>

## S100A12

The human S100A12 homodimer houses two His<sub>3</sub>Asp sites at the dimer interface that are composed of residues His15 and Asp25 of one subunit, and His85' and His89' of the other subunit (Figure 2D–F). Five crystal structures of S100A12 have been reported to date, including a structure of the Zn(II)-bound protein.<sup>49–53</sup> In this structure, each Zn(II) ion is coordinated at a His<sub>3</sub>Asp site in a distorted tetrahedral geometry, affording a 2:1 Zn(II):S100A12 stoichiometry.<sup>49</sup> On the basis of crystallographic and solution studies, S100A12 exhibits complex oligomerization behavior.<sup>49–53</sup> For instance, Zn(II) binding causes two S100A12 dimers to self-associate into tetramers, and coordination of both Ca(II) and Zn(II) results in the formation of hexamers.<sup>49,50</sup> We note that a crystal structure of Cu(II)-bound S100A12 shows a 2:1 Cu(II):S100A12 stoichiometry where the Cu(II) ions bind at the His<sub>3</sub> Asp sites.<sup>50,51</sup> It was also hypothesized that the interplay between S100A12 and Cu(II) contributes to the anti-parasitic activity of S100A12;<sup>76</sup> however, to the best of our knowledge, there is no reported experimental evidence that supports this notion. Further investigations are required to evaluate Cu(II) binding by S100A12 in solution and decipher its biological significance.

The crystal structure of Zn(II)-bound S100A12 provided a foundation for recent solution studies addressing its Zn(II)-chelating properties. Zn(II) competition experiments with a series of small-molecule Zn(II) sensors, including the fluorescent Zn(II) sensor FZ3 ( $K_{d,Zn(II)} = 9$  nM, pH 7.4),<sup>77</sup> established that human S100A12 binds Zn(II) with subnanomolar affinity (Table 1).<sup>55</sup> These results are reminiscent of early studies of porcine S100A12, which reported that this orthologue binds Zn(II) tightly ( $K_{d,Zn(II)} = 10$  nM),<sup>42</sup> and refute a prior study that employed intrinsic protein emission to study human S100A12 and reported  $K_{d,Zn(II)}$  values of  $>10$   $\mu$ M for each site.<sup>49</sup> Although further work is required to determine the  $K_{d,Zn(II)}$  values of S100A12 and determine how Ca(II) ions affect Zn(II) binding, the current data are consistent with the notion that S100A12 functions as a Zn(II)-sequestering protein. Moreover, results from several other experiments indicated that Ca(II)-bound S100A12 has higher Zn(II) affinity than the apo protein. For instance, selective Zn(II) depletion from microbial growth medium by S100A12 was enhanced when the medium was

supplemented with  $\approx 2$  mM Ca(II).<sup>55</sup> Moreover, the antimicrobial activity of S100A12 was enhanced in the presence of excess Ca(II) ions.<sup>55</sup> These observations support the notion that Ca(II) ions modulate the functional properties of S100A12 such that its Zn(II)-sequestering ability is enhanced in the extracellular space.

Indeed, several recent reports provide compelling evidence that S100A12 functions as a Zn(II)-withholding protein. One investigation revealed that S100A12 is more prevalent within *Helicobacter pylori*-infected gastric tissue compared to healthy tissue, and S100A12 was shown to inhibit the growth of *H. pylori* through a Zn(II)-reversible mechanism.<sup>54</sup> Another report identified S100A12 as an antifungal agent that displays Ca(II)-dependent growth inhibitory activity against *Candida* spp.<sup>55</sup> The antifungal activity of S100A12 was lost when the protein was pre-incubated with two equivalents of Zn(II), supporting a Zn(II)-starvation mode of action.

Although both S100A12 and CP sequester Zn(II) and appear to have similar Ca(II) dependence, there are marked differences in the antimicrobial profiles of these proteins. S100A12 exhibits a relatively narrow spectrum of antimicrobial activity,<sup>55</sup> whereas CP provides growth inhibition against a variety of bacterial and fungal pathogens.<sup>27,28,68</sup> CP is functionally versatile because of its ability to sequester multiple first-row transition metals, which are essential nutrients, at the His<sub>6</sub> site. In contrast, S100A12 (and the His<sub>3</sub>Asp site of CP) is more selective and sequesters Zn(II) but not Mn(II), Fe(II) and Ni(II).<sup>55</sup> Thus, it is possible that microbes that are more sensitive to Zn(II) deprivation are more susceptible to S100A12.

Because neutrophils produce and release S100A12 and CP, it is likely that these two proteins act together in the extracellular space. Metal substitution experiments with CP indicate that the His<sub>6</sub> site binds a divalent transition metal rapidly and with slow exchange, and that it will entrap the metal it encounters first.<sup>37</sup> Given that Zn(II) is ubiquitous and relatively abundant, we propose that Zn(II) sequestration by S100A12 may boost the ability of CP to capture other nutrient metals like Fe(II), Mn(II), and Ni(II) at the His<sub>6</sub> site.<sup>55</sup> Most studies consider S100A12 and CP independently, and investigating these two proteins together may improve our understanding of metal sequestration by the host innate immune system.

### S100A7 (Psoriasin)

The human S100A7 homodimer contains two His<sub>3</sub>Asp motifs at the dimer interface.<sup>58,59</sup> These Zn(II)-binding sites are composed of His87 and His91 from one monomer, and His18' and Asp25' from the other monomer (Figure 2G–I, Figure 3).<sup>58,59</sup> Two crystal structures of Zn(II)-bound S100A7 have been reported and both show a 2:1 Zn(II):S100A7 stoichiometry with each Zn(II) ion coordinated at a His<sub>3</sub>Asp site in a distorted tetrahedral geometry.<sup>59</sup>

S100A7 has several unusual structural attributes. Its N-terminal EF-hand is truncated; thus, the loop is three residues shorter than the corresponding loops of S100A12 and CP (Figure 3). The N-terminal EF hand also contains a Ser residue at position 30. This position corresponds to an Asp/Glu residue that binds Ca(II) in S100A12, S100A8, and S100A9 (Figure 3). Another striking structural feature of S100A7 is that each polypeptide contains

two Cys residues, Cys47 and Cys96, which can form an intramolecular disulfide bond (Figures 2, 3).<sup>58, 59</sup> As a result, the S100A7 homodimer can exist in the reduced form (S100A7<sub>red</sub>) with four free Cys thiolates or in the oxidized form (S100A7<sub>ox</sub>) with two intramolecular disulfide bonds. Moreover, the Cys47–Cys96 disulfide bond is in close proximity to the Zn(II)-binding motifs; Cys96 is separated from the Zn(II)-coordinating residue His91 by a Gly-Ala-Ala-Pro loop. These structural features motivated examination of the effects of disulfide bond formation and Ca(II) ions on the Zn(II)-binding properties and antibacterial activity of S100A7.<sup>64</sup> Investigation of the disulfide redox behavior of S100A7 revealed that (i) the midpoint potential of S100A7 falls in the physiological range; (ii) Ca(II) binding depresses the midpoint potential by 40 mV from –255 mV for the apo protein to –298 mV for the Ca(II)-bound protein at pH 7.0; (iii) Zn(II) coordination appears to further depress the midpoint potential such that the value cannot be determined using standard redox buffer systems, (iv) apo S100A7<sub>ox</sub> is a substrate for the mammalian thioredoxin system (Trx/TrxR), and (v) metal-bound S100A7<sub>ox</sub> is not readily reduced by Trx/TrxR.<sup>64</sup> Taken together, these observations indicated that both S100A7<sub>ox</sub> and S100A7<sub>red</sub> can exist under physiological conditions, and that metal-bound S100A7 is more likely to be in the oxidized form. The former conclusion is in agreement with prior *ex vivo* analyses that reported the isolation of S100A7<sub>ox</sub> and S100A7<sub>red</sub> from skin samples.<sup>60,63</sup>

Zn(II) competition experiments demonstrated that S100A7<sub>ox</sub> and S100A7<sub>red</sub> each coordinate two equivalents of Zn(II) with sub-nanomolar affinity in the absence and presence of Ca(II) ions (Table 1), and that the cysteine thiolates in S100A7<sub>red</sub> do not form a third high-affinity Zn(II) site.<sup>64</sup> This work provided revision to a previously reported  $K_{d,Zn(II)}$  value for S100A7 of 100  $\mu$ M.<sup>57</sup> The results also refuted a prior hypothesis that a third high-affinity Zn(II)-binding site created by the Cys thiolates conferred antifungal activity to S100A7<sub>red</sub>.<sup>63</sup> Moreover, Zn(II) competition titrations with ZP4<sup>72</sup> revealed similar  $K_{d,Zn(II)}$  values for S100A7<sub>ox</sub> and S100A7<sub>red</sub> in both the absence and presence of excess Ca(II) ions (Table 1). These results indicated that (i) the redox state of the Cys residues in S100A7 has a negligible effect on the apparent  $K_{d,Zn(II)}$  value obtained using ZP4, and (ii) apo- and Ca(II)-bound S100A7 have similar Zn(II) affinities. The latter observation indicates that S100A7 does not share the same Ca(II) dependence as CP and S100A12.

Although the Zn(II) competition studies described above revealed negligible difference in Zn(II) affinities of S100A7<sub>red</sub> and S100A7<sub>ox</sub>, several other lines of experimental evidence indicated that S100A7<sub>ox</sub> is more effective at Zn(II) sequestration than S100A7<sub>red</sub>. For instance, experiments that probed metal exchange at the His<sub>3</sub>Asp sites demonstrated that the metal substitution rate occurs more slowly for S100A7<sub>ox</sub> than S100A7<sub>red</sub>. Moreover, investigations of antibacterial activity showed that S100A7<sub>ox</sub> is more active than S100A7<sub>red</sub>.<sup>64</sup> In total, these results suggested that S100A7 can exist in more than one form depending on the redox environment and presence of divalent cations like Ca(II) and Zn(II). In addition, it appears that S100A7 uses redox cues to tune its Zn(II)-sequestering ability and antibacterial activity, and that S100A7<sub>ox</sub> may be a more important contributor to Zn(II) withholding in the extracellular space than S100A7<sub>red</sub>. We expect that further biophysical studies designed to elucidate how disulfide bond formation and reduction affects the protein scaffold and Zn(II) coordination at the His<sub>3</sub>Asp sites will be informative.

## Outlook

Over the past decade, our understanding of how the host and pathogen compete for Zn(II) and other essential metal nutrients has markedly advanced, and S100 proteins have emerged as key players in the metal-withholding innate immune response. The remarkable coordination chemistry exhibited by human CP, S100A12, and S100A7 provides new examples of how metal-binding properties can be tuned by environmental cues. Studies of Zn(II) chelation by CP revealed that Ca(II) binding enhances the Zn(II) affinity of this protein, and provided a paradigm for considering how Ca(II) ions affect its ability to sequester other metal nutrients as well as its antimicrobial activity. Subsequent investigations of Zn(II) sequestration by S100A12 and S100A7 built upon this work and afforded some similarities as well as striking differences, highlighting that metal-sequestering S100 proteins must be evaluated on a case-by-case basis. Similar to CP, current work indicates that Ca(II) ions modulate the Zn(II)-binding affinity of S100A12 and that this protein has the capacity to sequester Zn(II) in the extracellular space. S100A7, in contrast, appears to tune its Zn(II)-sequestering capacity through intramolecular disulfide-bond redox chemistry. Curiously, the disulfide bonds of S100A7 are more difficult to reduce when the protein is Ca(II) bound, which suggests an indirect modulatory effect of Ca(II) ions on the Zn(II)-binding properties of this protein. Taken together, a compelling picture emerges where CP, S100A12 and S100A7 are exquisitely designed to limit Zn(II) availability in the extracellular space.

From a physiological perspective, these three S100 proteins are abundant and involved in Zn(II) homeostasis and innate immunity. They are also implicated in other pathological processes that include the inflammatory response and tumorigenesis.<sup>11</sup> In order to fully appreciate how CP, S100A12 and S100A7 contribute to human physiology and pathology in broad terms and understand whether the Zn(II)-bound forms are important players, it is essential to understand the molecular underpinnings of Zn(II) coordination by each protein. In closing, we believe that the three case studies illustrated in this perspective convey the importance of deciphering the interplay between Zn(II) and S100 proteins at the host/pathogen interface from the fundamental and molecular perspectives, and provide a foundation for further refining current models that describe how S100 proteins contribute to Zn(II) biology.

## Acknowledgments

### Funding Source Statement

Our current studies of Zn(II) and S100 proteins are supported by the NSF (CHE-1352132) and the NIH (R01GM118695).

## References

1. Vallee BL, Falchuk KH. The biochemical basis of zinc physiology. *Physiol Rev.* 1993; 73:79–118. [PubMed: 8419966]
2. Andreini C, Banci L, Bertini I, Rosato A. Zinc through the three domains of life. *J Proteome Res.* 2006; 5:3173–3178. [PubMed: 17081069]

3. Wilson D. An evolutionary perspective on zinc uptake by human fungal pathogens. *Metallomics*. 2015; 7:979–985. [PubMed: 25652414]
4. Capdevila DA, Wang J, Giedroc DP. Bacterial strategies to maintain zinc metallostasis at the host-pathogen interface. *J Biol Chem*. 2016; 291:20858–20868. [PubMed: 27462080]
5. Braymer JJ, Giedroc DP. Recent developments in copper and zinc homeostasis in bacterial pathogens. *Curr Opin Chem Biol*. 2014; 19:59–66. [PubMed: 24463765]
6. Weinberg ED. Nutritional immunity: Host's attempt to withhold iron from microbial invaders. *J Am Med Assoc*. 1975; 231:39–41.
7. Hood MI, Skaar EP. Nutritional immunity: transition metals at the pathogen-host interface. *Nat Rev Microbiol*. 2012; 10:525–537. [PubMed: 22796883]
8. Zackular JP, Chazin WJ, Skaar EP. Nutritional immunity: S100 proteins at the host-pathogen interface. *J Biol Chem*. 2015; 290:18991–18998. [PubMed: 26055713]
9. Hantke K. Bacterial zinc uptake and regulators. *Curr Opin Microbiol*. 2005; 8:196–202. [PubMed: 15802252]
10. Jung WH. The zinc transport systems and their regulation in pathogenic fungi. *Mycobiology*. 2015; 43:179–183. [PubMed: 26539032]
11. Donato R, Canon BR, Sorci G, Riuzzi F, Hsu K, Weber DJ, Geczy CL. Functions of S100 proteins. *Curr Mol Med*. 2013; 13:24–57. [PubMed: 22834835]
12. Gifford JL, Walsh MP, Vogel HJ. Structures and metal-ion-binding properties of the Ca<sup>2+</sup>-binding helix-loop-helix EF-hand motifs. *Biochem J*. 2007; 405:199–221. [PubMed: 17590154]
13. Wilkinson MM, Busuttill A, Hayward C, Brock DJH, Dorin JR, Van Heyningen V. Expression pattern of two cystic fibrosis-associated calcium-binding proteins in normal and abnormal tissues. *J Cell Sci*. 1988; 91:221–230. [PubMed: 3267695]
14. Steinbakk M, Naess-Andresen C-F, Fagerhol MK, Lingaas E, Dale I, Brandtzaeg P. Antimicrobial actions of calcium binding leukocyte L1 protein, calprotectin. *Lancet*. 1990; 336:763–765. [PubMed: 1976144]
15. Teigelkamp S, Bharwaj RS, Roth J, Meinardus-Harger G, Karas MSC. Calcium-dependent complex assembly of the myeloid differentiation proteins MRP-8 and MRP-14. *J Biol Chem*. 1991; 266:13462–13467. [PubMed: 2071612]
16. Nacken W, Roth J, Sorg C, Kerkhoff C. S100A9/S100A8: Myeloid representatives of the S100 protein family as prominent players in innate immunity. *Microsc Res Tech*. 2003; 60:569–580. [PubMed: 12645005]
17. Vogl T, Roth J, Sorg C, Hillenkamp F, Strupat K. Calcium-induced noncovalently linked tetramers of MRP8 and MRP14 detected by ultraviolet matrix-assisted laser desorption/ionization mass spectrometry. *J Am Soc Mass Spectrom*. 1999; 10:1124–1130. [PubMed: 10536818]
18. Strupat K, Rogniaux H, Van Dorsselaer A, Roth J, Vogl T. Calcium-induced noncovalently linked tetramers of MRP8 and MRP14 are confirmed by electrospray ionization-mass analysis. *J Am Soc Mass Spectrom*. 2000; 11:780–788. [PubMed: 10976885]
19. Leukert N, Vogl T, Strupat K, Reichelt R, Sorg C, Roth J. Calcium-dependent tetramer formation of S100A8 and S100A9 is essential for biological activity. *J Mol Biol*. 2006; 359:961–972. [PubMed: 16690079]
20. Korndörfer IP, Brueckner F, Skerra A. The crystal structure of the human (S100A8/S100A9)<sub>2</sub> heterotetramer, calprotectin, illustrates how conformational changes of interacting  $\alpha$ -helices can determine specific association of two EF-hand proteins. *J Mol Biol*. 2007; 370:887–898. [PubMed: 17553524]
21. Stephan JR, Nolan EM. Calcium-induced tetramerization and zinc chelation shield human calprotectin from degradation by host and bacterial extracellular proteases. *Chem Sci*. 2016; 7:1962–1975. [PubMed: 26925211]
22. Sohnle PG, Collins-Lech C, Wiessner JH. The zinc-reversible antimicrobial activity of neutrophil lysates and abscess fluid supernatants. *J Infect Dis*. 1991; 164:137–142. [PubMed: 2056200]
23. Murthy ARK, Lehrer RI, Harwig SSL, Miyasaki KT. In vitro candidastatic properties of the human neutrophil calprotectin complex. *J Immunol*. 1993; 151:6291–6301. [PubMed: 8245468]

24. Miyasaki KT, Bodeau AL, Murthy ARK, Lehrer RI. In vitro antimicrobial activity of the human neutrophil cytosolic S-100 protein complex, calprotectin, against *Capnocytophaga sputigena*. *J Dent Res*. 1993; 72:517–523. [PubMed: 8423249]
25. Clohessy PA, Golden BE. Calprotectin-mediated zinc chelation as a biostatic mechanism in host-defense. *Scand J Immunol*. 1995; 42:551–556. [PubMed: 7481561]
26. Clohessy PA, Golden BE. His-X-X-X-His motif in S100 protein, calprotectin: Relation to microbiostatic activity. *J Leukoc Biol*. 1996; 60:674. [PubMed: 8929560]
27. Brophy MB, Hayden JA, Nolan EM. Calcium ion gradients modulate the zinc affinity and antibacterial activity of human calprotectin. *J Am Chem Soc*. 2012; 134:18089–18100. [PubMed: 23082970]
28. Nakashige TG, Stephan JR, Cunden LS, Brophy MB, Wommack AJ, Keegan BC, Shearer JM, Nolan EM. The hexahistidine motif of host-defense protein human calprotectin contributes to zinc withholding and its functional versatility. *J Am Chem Soc*. 2016; 138:12243–12251. [PubMed: 27541598]
29. Liu JZ, Jellbauer S, Poe AJ, Ton V, Pesciaroli M, Kehl-Fie TE, Restrepo NA, Hosking MP, Edwards RA, Battistoni A, Pasquali P, Lane TE, Chazin WJ, Vogl T, Roth J, Skaar EP, Raffatellu M. Zinc sequestration by the neutrophil protein calprotectin enhances *Salmonella* growth in the inflamed gut. *Cell Host Microbe*. 2012; 11:227–239. [PubMed: 22423963]
30. Hood MI, Mortensen BL, Moore JL, Zhang Y, Kehl-Fie TE, Sugitani N, Chazin WJ, Caprioli RM, Skaar EP. Identification of an *Acinetobacter baumannii* zinc acquisition system that facilitates resistance to calprotectin-mediated zinc sequestration. *PLoS Pathog*. 2012; 8:e1003068. [PubMed: 23236280]
31. Mortensen BL, Rathi S, Chazin WJ, Skaar EP. *Acinetobacter baumannii* response to host-mediated zinc limitation requires the transcriptional regulator Zur. *J Bacteriol*. 2014; 196:2616–2626. [PubMed: 24816603]
32. Nairn BL, Lonergan ZR, Wang J, Braymer JJ, Zhang Y, Calcutt MW, Lisher JP, Gilston BA, Chazin WJ, de Crécy-Lagard V, Giedroc DP, Skaar EP. The response of *Acinetobacter baumannii* to zinc starvation. *Cell Host Microbe*. 2016; 19:826–836. [PubMed: 27281572]
33. Stork M, Grijpstra J, Bos MP, Torres CM, Devos N, Poolman JT, Chazin WJ, Tommassen J. Zinc piracy as a mechanism of *Neisseria meningitidis* for evasion of nutritional immunity. *PLoS Pathog*. 2013; 9:e1003733. [PubMed: 24204275]
34. Corbin BD, Seeley EH, Raab A, Feldmann J, Miller MR, Torres VJ, Anderson KL, Dattilo BM, Dunman PM, Gerads R, Caprioli RM, Nacken W, Chazin WJ, Skaar EP. Metal chelation and inhibition of bacterial growth in tissue abscesses. *Science*. 2008; 319:962–965. [PubMed: 18276893]
35. Kehl-Fie TE, Chitayat S, Hood MI, Damo S, Restrepo N, Garcia C, Munro KA, Chazin WJ, Skaar EP. Nutrient metal sequestration by calprotectin inhibits bacterial superoxide defense, enhancing neutrophil killing of *Staphylococcus aureus*. *Cell Host Microbe*. 2011; 10:158–164. [PubMed: 21843872]
36. Hadley RC, Gagnon DM, Brophy MB, Gu Y, Nakashige TG, Britt RD, Nolan EM. Biochemical and spectroscopic observation of Mn(II) sequestration from bacterial Mn(II) transport machinery by calprotectin. *J Am Chem Soc*. 2018; 140
37. Nakashige TG, Zhang B, Krebs C, Nolan EM. Human calprotectin is an iron-sequestering host-defense protein. *Nat Chem Biol*. 2015; 11:765–771. [PubMed: 26302479]
38. Nakashige TG, Zygiel EM, Drennan CL, Nolan EM. Nickel sequestration by the host-defense protein human calprotectin. *J Am Chem Soc*. 2017; 139:8828–8836. [PubMed: 28573847]
39. Besold AN, Gilston BA, Radin JN, Ramsoomair C, Culbertson EM, Li CX, Cormack BP, Chazin WJ, Kehl-Fie TE, Culotta VC. The role of calprotectin in withholding zinc and copper from *Candida albicans*. *Infect Immun*. 2017; 86:e00779–00717.
40. Guignard F, Mauel J, Markert M. Identification and characterization of a novel human neutrophil protein related to the S100 family. *Biochem J*. 1995; 309:395–401. [PubMed: 7626002]
41. Ilg EC, Troxler H, Bürgisser DM, Kuster T, Markert M, Guignard F, Hunziker P, Birchler N, Heizmann CW. Amino acid sequence determination of human S100A12 (P6, calgranulin C,

- CGRP, CAAF1) by tandem mass spectrometry. *Biochem Biophys Res Commun.* 1996; 225:146–150. [PubMed: 8769108]
42. Dell'Angelica EC, Schleicher CH, Santomé JA. Primary structure and binding properties of calgranulin C, a novel S100-like calcium-binding protein from pig granulocytes. *J Biol Chem.* 1994; 269:28929–28936. [PubMed: 7961855]
43. Hitomi J, Kimura T, Kusumi E, Nakagawa S, Kuwabara S, Hatakeyama K, Yamaguchi K. Novel S100 proteins in human esophageal epithelial cells: CAAF1 expression is associated with cell growth arrest. *Arch Histol Cytol.* 1998; 61:163–178. [PubMed: 9650890]
44. Yang Z, Tao T, Raftery MJ, Youssef P, Di Girolamo N, LGC. Proinflammatory properties of the human S100 protein S100A12. *J Leukoc Biol.* 2001; 69:986–994. [PubMed: 11404386]
45. Robinson MJ, Hogg N. A comparison of human S100A12 with MRP-14 (S100A9). *Biochem Biophys Res Commun.* 2000; 275:865–870. [PubMed: 10973813]
46. Foell D, Kucharzik T, Kraft M, Vogl T, Sorg C, Domschke W, Roth J. Neutrophil derived human S100A12 (EN-RAGE) is strongly expressed during chronic active inflammatory bowel disease. *Gut.* 2003; 52:847–853. [PubMed: 12740341]
47. Foell D, Hernández-Rodríguez J, Sánchez M, Vogl T, Cid MC, Roth J. Early recruitment of phagocytes contributes to the vascular inflammation of giant cell arteritis. *J Pathol.* 2004; 204:311–316. [PubMed: 15476267]
48. Yang Z, Yan WX, Cai H, Tedla N, Armishaw C, Di Girolamo N, Wang HW, Hampartzoumian T, Simpson JL, Gibson PG, Hunt J, Hart P, Hughes JM, Perry MA, Alewood PF, Geczy CL. S100A12 provokes mast cell activation: a potential amplification pathway in asthma and innate immunity. *J Allergy Clin Immunol.* 2007; 119:106–114. [PubMed: 17208591]
49. Moroz OV, Burkitt W, Wittkowski H, He W, Ianoul A, Novitskaya V, Xie J, Polyakova O, Lednev IK, Shekhtman A, Derrick PJ, Bjoerk P, Foell D, Bronstein IB. Both Ca<sup>2+</sup> and Zn<sup>2+</sup> are essential for S100A12 protein oligomerization and function. *BMC Biochem.* 2009; 10:11. [PubMed: 19386136]
50. Moroz OV, Dodson GG, Wilson KS, Lukanidin E, Bronstein IB. Multiple structural states of S100A12: A key to its functional diversity. *Microsc Res Tech.* 2003; 60:581–592. [PubMed: 12645006]
51. Moroz OV, Antson AA, Grist SJ, Maitland NJ, Dodson GG, Wilson KS, Lukanidin E, Bronstein IB. Structure of the human S100A12-copper complex: implications for host-parasite defence. *Acta Crystallogr D Biol Crystallogr.* 2003; 59:859–867. [PubMed: 12777802]
52. Moroz OV, Antson AA, Dodson EJ, Burrell HJ, Grist SJ, Lloyd RM, Maitland NJ, Dodson GG, Wilson KS, Lukanidin E, Bronstein IB. The structure of S100A12 in a hexameric form and its proposed role in receptor signalling. *Acta Crystallogr D Biol Crystallogr.* 2002; 58:407–413. [PubMed: 11856825]
53. Moroz OV, Antson AA, Murshudov GN, Maitland NJ, Dodson GG, Wilson KS, Skibshøj I, Lukanidin EM, Bronstein IB. The three-dimensional structure of human S100A12. *Acta Crystallogr D Biol Crystallogr.* 2001; 57:20–29. [PubMed: 11134923]
54. Haley KP, Delgado AG, Piazuolo MB, Mortensen BL, Correa P, Damo SM, Chazin WJ, Skaar EP, Gaddy JA. The human antimicrobial protein calgranulin C participates in control of *Helicobacter pylori* growth and regulation of virulence. *Infect Immun.* 2015; 83:2944–2956. [PubMed: 25964473]
55. Cunden LS, Gaillard A, Nolan EM. Calcium ions tune the zinc-sequestering properties and antimicrobial activity of human S100A12. *Chem Sci.* 2016; 7:1338–1348. [PubMed: 26913170]
56. Jinquan T, Vorum H, Larsen CG, Madsen P, Rasmussen HH, Gesser B, Etzerodt M, Honoré B, Celis JE, Thestrup-Pedersen K. Psoriasin: A novel chemotactic protein. *J Invest Dermatol.* 1996; 107:5–10. [PubMed: 8752830]
57. Vorum H, Madsen P, Rasmussen HH, Etzerodt M, Svendsen I, Celis JE, Honoré B. Expression and divalent cation binding properties of the novel chemotactic inflammatory protein psoriasin. *Electrophoresis.* 1996; 17:1787–1796. [PubMed: 8982613]
58. Brodersen DE, Etzerodt M, Madsen P, Celis JE, Thøgersen HC, Nyborg J, Kjeldgaard M. EF-hands at atomic resolution: the structure of human psoriasin (S100A7) solved by MAD phasing. *Structure.* 1998; 6:477–489. [PubMed: 9562557]

59. Brodersen DE, Nyborg J, Kjeldgaard M. Zinc-binding site of an S100 protein revealed. Two crystal structures of Ca<sup>2+</sup>-bound human psoriasin (S100A7) in the Zn<sup>2+</sup>-loaded and Zn<sup>2+</sup>-free states. *Biochemistry*. 1999; 38:1695–1704. [PubMed: 10026247]
60. Gläser R, Harder J, Lange H, Bartels J, Christophers E, Schröder J-M. Antimicrobial psoriasin (S100A7) protects human skin from *Escherichia coli* infection. *Nat Immunol*. 2005; 6:57–64. [PubMed: 15568027]
61. Meyer JE, Harder J, Sipos B, Maune S, Klöppel G, Bartels J, Schröder JM, Gläser R. Psoriasin (S100A7) is a principal antimicrobial peptide of the human tongue. *Mucosal Immunol*. 2008; 1:239–243. [PubMed: 19079183]
62. Mildner M, Stichenwirth M, Abtin A, Eckhart L, Sam C, Gläser R, Schröder J-M, Gmeiner R, Mlitz V, Pammer J, Geusau A, Tschachler E. Psoriasin (S100A7) is a major *Escherichia coli*-cidal factor of the female genital tract. *Mucosal Immunol*. 2010; 127:602–609.
63. Hein KZ, Takahashi H, Tsumori T, Yasui Y, Nanjoh Y, Toga T, Wu Z, Grötzinger J, Jung S, Wehkamp J, Schroeder BO, Schroeder JM, Morita E. Disulphide-reduced psoriasin is a human apoptosis-inducing broad-spectrum fungicide. *Proc Natl Acad Sci U S A*. 2015; 112:13039–13044. [PubMed: 26438863]
64. Cunden LS, Brophy MB, Rodriguez GE, Flaxman HA, Nolan EM. Biochemical and functional evaluation of the intramolecular disulfide bonds in the zinc-chelating antimicrobial protein human S100A7 (Psoriasin). *Biochemistry*. 2017; 56:5726–5738. [PubMed: 28976190]
65. Donato R. Functional roles of S100 proteins, calcium-binding proteins of the EF-hand type. *Biochim Biophys Acta*. 1999:191–231.
66. Goyette J, Geczy CL. Inflammation-associated S100 proteins: new mechanisms that regulate function. *Amino Acids*. 2011; 41:821–842. [PubMed: 20213444]
67. Xie J, Burz DS, He W, Bronstein IB, Lednev I, Shekhtman A. Hexameric calgranulin C (S100A12) binds to the receptor for advanced glycated end products (RAGE) using symmetric hydrophobic target-binding patches. *J Biol Chem*. 2007; 282:4218–4231. [PubMed: 17158877]
68. Damo SM, Kehl-Fie TE, Sugitani N, Holt ME, Rathi S, Murphy WJ, Zhang Y, Betz C, Hench L, Fritz G, Skaar EP, Chazin WJ. Molecular basis for manganese sequestration by calprotectin and roles in the innate immune response to invading bacterial pathogens. *Proc Natl Acad Sci U S A*. 2013; 110:3841–3846. [PubMed: 23431180]
69. Brophy MB, Nakashige TG, Gaillard A, Nolan EM. Contributions of the S100A9 C-terminal tail to high-affinity Mn(II) chelation by the host-defense protein human calprotectin. *J Am Chem Soc*. 2013; 135:17804–17817. [PubMed: 24245608]
70. Gagnon DM, Brophy MB, Bowman SE, Stich TA, Drennan CL, Britt RD, Nolan EM. Manganese binding properties of human calprotectin under conditions of high and low calcium: X-ray crystallographic and advanced electron paramagnetic resonance spectroscopic analysis. *J Am Chem Soc*. 2015; 137:3004–3016. [PubMed: 25597447]
71. Gazaryan IG, Krasnikov BF, Ashby GA, Thorneley RNF, Kristal BS, Brown AM. Zinc is a potent inhibitor of thiol oxidoreductase activity and stimulates reactive oxygen species production by lipoamide dehydrogenase. *J Biol Chem*. 2002; 277:10064–10072. [PubMed: 11744691]
72. Burdette SC, Frederickson CJ, Bu WM, Lippard SJ. ZP4, an improved neuronal Zn<sup>2+</sup> sensor of the Zinpyr family. *J Am Chem Soc*. 2003; 125:1778–1787. [PubMed: 12580603]
73. Kwon JE, Lee S, You Y, Baek K-H, Ohkubo K, Cho J, Fukuzumi S, Shin I, Park SY, Nam W. Fluorescent zinc sensor with minimized proton-induced interferences: photophysical mechanism for fluorescence turn-on response and detection of endogenous free zinc ions. *Inorg Chem*. 2012; 51:8760–8774. [PubMed: 22534151]
74. Hayden JA, Brophy MB, Cunden LS, Nolan EM. High-affinity manganese coordination by human calprotectin is calcium-dependent and requires the histidine-rich site formed at the dimer interface. *J Am Chem Soc*. 2013; 135:775–787. [PubMed: 23276281]
75. Sohnle PG, Collins-Lech C, Wiessner JH. Antimicrobial activity of an abundant calcium-binding protein in the cytoplasm of human neutrophils. *J Infect Dis*. 1991; 163:187–192. [PubMed: 1984467]
76. Gottsch JD, Eisinger SW, Liu SH, LSA. Calgranulin C has filariacidal and filariastatic activity. *Infect Immun*. 1999; 67:6631–6636. [PubMed: 10569784]

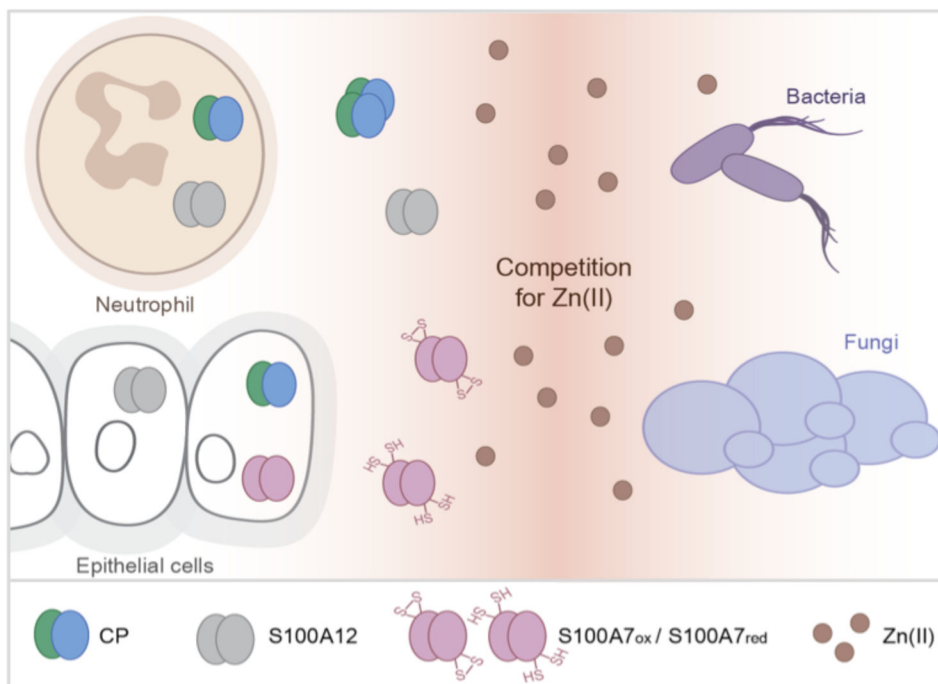
77. Kręgiel A, Maret W. Dual nanomolar and picomolar Zn(II) binding properties of metallothionein. *J Am Chem Soc.* 2007; 129:10911–10921. [PubMed: 17696343]

Author Manuscript

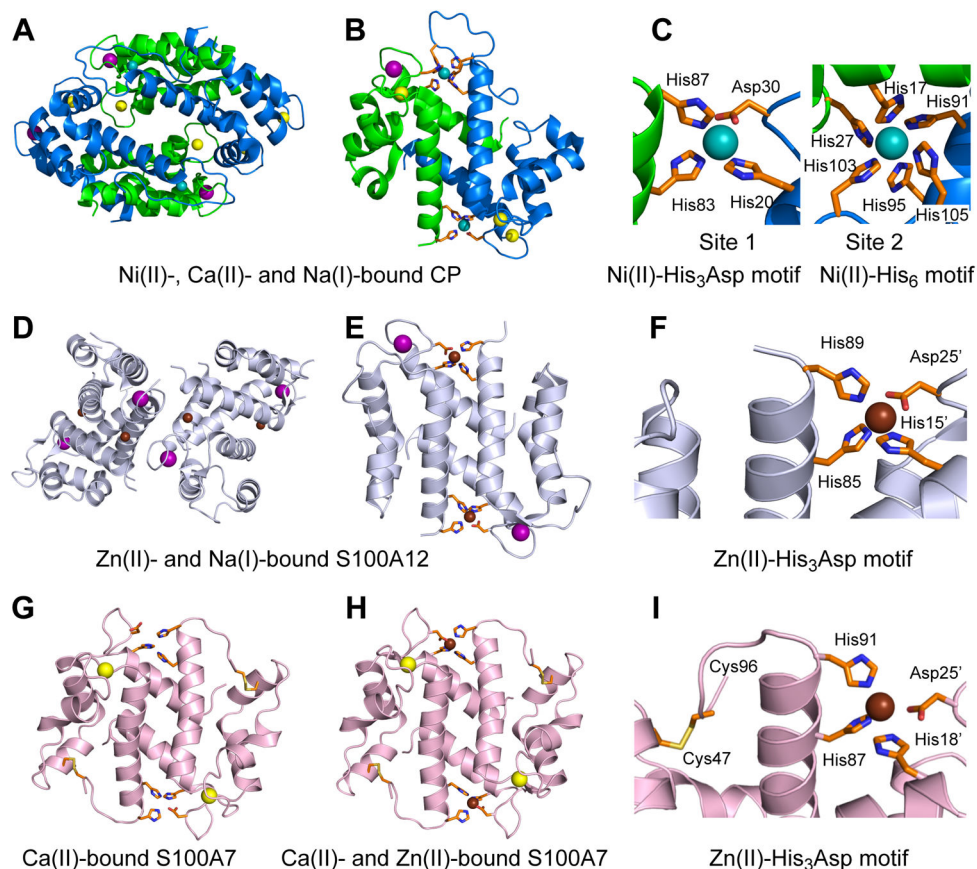
Author Manuscript

Author Manuscript

Author Manuscript



**Figure 1.** Extracellular roles of CP, S100A12, and S100A7 in Zn(II) sequestration. Neutrophils, other types of white blood cells including monocytes and macrophages (not shown), and epithelial cells release these host-defense proteins into the extracellular space as described in the cartoon and main text. These proteins compete with microbes for bioavailable Zn(II) in the extracellular space.

**Figure 2.**

Crystal structures of human CP, S100A12, and S100A7. (A, B) Structure of Ni(II)-, Ca(II)- and Na(I)-bound CP heterotetramer and a heterodimer unit taken from this structure that shows the transition-metal-binding sites (PDB 5W1F). (C) Zoom-in view showing the His<sub>3</sub>Asp (Site 1) and His<sub>6</sub> (Site 2) motifs of CP (PDB 5W1F). (D, E) Structure of Zn(II)- and Na(I)-bound S100A12 tetramer and a dimer unit of this structure that shows the transition-metal-binding sites (PDB 2WC8). (F) Zoom-in view showing the His<sub>3</sub>Asp motif of S100A12 (PDB 2WC8). (G) Ca(II)-bound structure of S100A7 dimer (PDB 3PSR). (H) Zn(II)- and Ca(II)-bound structure of S100A7 dimer (PDB 2PSR). (I) Zoom-in view showing the His<sub>3</sub>Asp motif of S100A7 (PDB 2PSR). Zn(II), Ni(II), Ca(II), and Na(I) ions are shown as brown, teal, yellow, and purple spheres, respectively.

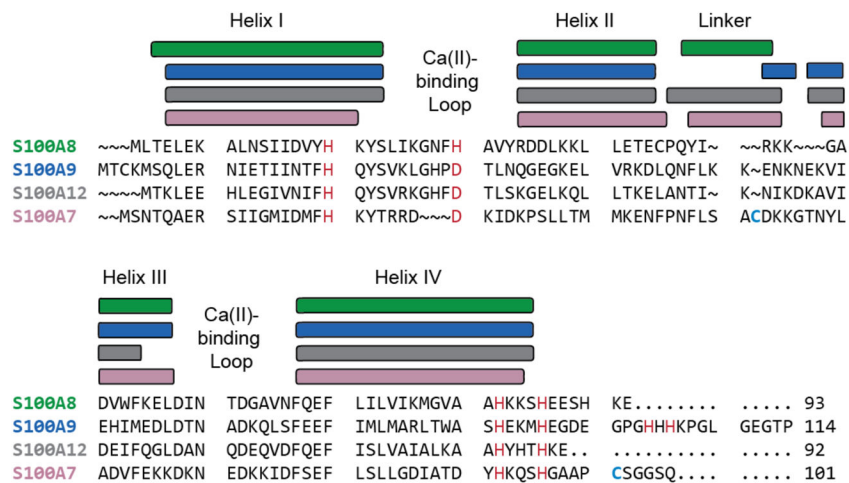


**Figure 3.** Sequence alignment of human S100A8, S100A9, S100A12, and S100A7. Secondary structural elements are presented above the alignment. The transition-metal-binding residues are presented in red, and Cys47 and Cys96 of S100A7 are highlighted in blue.

Table 1

Reported Apparent Dissociation Constant Values ( $K_{d,Zn(II)}$ ) for Human S100 Proteins.

Protein	$K_{d,Zn(II)}$	Method	Buffer conditions	Ref.
CP	1.4 nM 5.6 nM	ITC <sup>a</sup>	20 mM Tris, 100 mM NaCl, pH 7.5 stoichiometric Ca(II) <sup>b,c</sup>	35
CP-Ser <sup>d</sup>	133 ± 58 pM 185 ± 219 nM 10 pM <sup>e</sup> 240 pM <sup>e</sup>	Competition <sup>f</sup>	75 mM HEPES, 100 mM NaCl, pH 7.5 75 mM HEPES, 100 mM NaCl, pH 7.5, 15 – 45 equivalents Ca(II)	27
	90 ± 366 fM 0.9 ± 1 pM	Competition <sup>g</sup>	75 mM HEPES, 100 mM NaCl, pH 7.0 50 equivalents Ca(II)	28
CP His <sub>3</sub> Asp variant <sup>h</sup>	3.4 ± 1.2 nM	ITC <sup>a</sup>	20 mM HEPES, 100 mM NaCl, pH 7.5 Stoichiometric Ca(II) <sup>b</sup>	68
CP His <sub>4</sub> Variant <sup>i</sup>	8.2 ± 1.5 nM	ITC <sup>a</sup>	20 mM HEPES, 100 mM NaCl, pH 7.5 Stoichiometric Ca(II) <sup>b</sup>	68
CP-Ser H103A/H104A/H105A variant	4 ± 0.8 pM 22 ± 3 pM	Competition <sup>g</sup>	75 mM HEPES, 100 mM NaCl, pH 7.0 50 equivalents Ca(II)	28
S100A12	16 μM 83 μM	Tyr fluorescence	25 mM Tris-HCl, pH 7.4 <sup>c</sup>	49
S100A12	9 nM	Competition <sup>j</sup>	75 mM HEPES, 100 mM NaCl, pH 7.0	55
S100A7	100 μM	Equilibrium dialysis	20 mM Tris, 150 mM KCl, pH 7.4 <sup>c</sup>	57
S100A7 <sub>ox</sub>	430 ± 13 pM	Competition <sup>f</sup>	75 mM HEPES, 100 mM NaCl, pH 7.0	64
	580 ± 40 pM	Competition <sup>f</sup>	75 mM HEPES, 100 mM NaCl, pH 7.0 100 equivalents Ca(II)	64
S100A7 <sub>red</sub>	660 ± 56 pM	Competition <sup>f</sup>	75 mM HEPES, 100 mM NaCl, pH 7.0	64
	420 ± 41 pM	Competition <sup>f</sup>	75 mM HEPES, 100 mM NaCl, pH 7.0 100 equivalents Ca(II)	64
S100A7-Ser <sup>k</sup>	700 ± 58 pM	Competition <sup>f</sup>	75 mM HEPES, 100 mM NaCl, pH 7.0	64
	370 ± 11 pM	Competition <sup>f</sup>	75 mM HEPES, 100 mM NaCl, pH 7.0 100 equivalents Ca(II)	64
S100A7-Ala <sup>l</sup>	500 ± 69 pM	Competition <sup>f</sup>	75 mM HEPES, 100 mM NaCl, pH 7.0	64
	490 ± 21 pM	Competition <sup>f</sup>	75 mM HEPES, 100 mM NaCl, pH 7.0 100 equivalents Ca(II)	64

<sup>a</sup> Isothermal titration calorimetry (ITC) experiments were performed at 30 °C. Stoichiometric Zn(II) binding was observed.

<sup>b</sup> The definition of stoichiometric Ca(II) relative to the CP concentration was not specified.

<sup>c</sup> Metal-buffer equilibrium is a variable when Tris buffer is employed for studies of Zn(II) binding because Tris binds Zn(II) with  $K_{d,Zn} = 10^{-4}$  M.  
71

<sup>d</sup> CP contains two native Cys residues that were mutated to Ser for these metal-binding studies. CP-Ser is a S100A8(C42S)/S100A9(C3S) variant.

<sup>e</sup> CP-Ser outcompetes ZP4 in the presence of Ca(II), and the  $K_{d,Zn(II)}$  values were reported as upper limits.

<sup>f</sup> Competition experiments were performed with Zinpyr-4 (ZP4) at 25 °C.

<sup>g</sup> Competition experiments were performed with HNBO-DPA at 25 °C. These titrations were complicated by outcompetition and error. The fM  $K_{d,Zn(II)}$  value is considered to be an upper limit and the pM  $K_{d,Zn(II)}$  value is considered to be an estimate. The values were not assigned to particular sites.

<sup>h</sup>A variant of CP that only contains the His<sub>6</sub> site.

<sup>i</sup>A variant of CP that only contains the His<sub>3</sub>Asp site.

<sup>j</sup>Competition experiments were performed with FluoZin-3 (FZ3) at 25 °C.

<sup>k</sup>A S100A7(C47S)(C96S) variant.

<sup>l</sup>A S100A7(C47A)(C96A) variant. To determine the  $K_{d,Zn(II)}$  values from competition experiments, the averaged data were fit to a two-site model where  $K_{d1} = K_{d2}$  and  $K_{d1} = K_{d2}$  for CP and S100A7, respectively.

Author Manuscript

Author Manuscript

Author Manuscript

Author Manuscript